Adsorption 11: 249–253, 2005

Study of Multicomponent Gas Adsorption into MSC5A by Chromatograph

KAZUYUKI CHIHARA*, YOSUKE KANEKO, TAKUYA TERAKADO AND HISASHI MIZUOCHI
Department of Industrial Chemistry, Meiji University, 1-1-1 Higashi-mita, Tama-ku, Kawasaki, Kanagawa, 214-8571, Japan
chihara@isc.meiji.ac.jp

Abstract. Perturbation chromatography with multi component gas carrier and non-equilibrium thermodynamics liner law was applied for discussion of the interference effect and the displacement effect on mass transfer in multi component gas adsorption. Moment analysis method and stop & go simulation method were utilized to obtain each mass transfer parameters of adsorbate gases. Dependency of micropore diffusion on amount adsorbed and correlation of micropore diffusion with chemical potential driving force for microporous adsorbent were confirmed. Cross effect in micropore diffusion was found.

Keywords: chromatograph, stop & go simulation, multi component gas

1. Introduction

The combination of chromatographic method and moment analysis of the response peaks is one of the useful techniques to study adsorption equilibrium and adsorption rate (Chihara et al., 1978). Perturbation chromatography with the mixed multi component adsorbate gas carrier (two adsorbates) has been applied to several studies on adsorption (Ruthven and Kumar, 1979; Kumar et al., 1982). In this work, perturbation chromatography with multi component gas carrier (two adsorbates with inert gas) and non-equilibrium thermodynamics liner law was applied for discussion of the interference effect and the displacement effect (those are cross effects) on mass transfer in multi component gas adsorption. Moment analysis method and stop & go simulation method were utilized to obtain each mass transfer parameters of adsorbate gases. Dependency of micropore diffusion on amount adsorbed and correlation of micropore diffusion with chemical potential driving force for microporous adsorbent were discussed. Also, cross effect were discussed. Ruthven already pointed the dependency of micropore diffusivity on amount adsorbed in single component adsorption (Ruthven, 1984). Tondeur et al. gave general background on multi component perturbation chromatography for the first moment only (Tondeur et al., 1996).

2. Experimental Method

2.1. Experimental Procedure and Conditions

The experimental apparatus was shown in Fig. 1. The apparatus was similar to a conventional gas chromatograph. Adsorbent particles (molecular sieving carbon 5A, 20/30 mesh, Japan Enviro Chemical Ltd.) were packed in a column (100 cm × 3 mm i.d.). Carrier gas was a mixture of two or three components among He, N_2, CH_4. Perturbation pulse was introduced into the carrier gas stream. Introduction of pulses was performed by 6-way valve. The pulse size was 1 cc, which meant injection period was 1.4 [sec]. Then pulse response was detected by TCD cell and by mass filter (Dycor quadrupole mass detector). Output signal of TCD was transmitted to a personal computer through RS232C. Also, pulse response was introduced to mass detector to get individual response of each component. These signals were also transmitted to the

---

*To whom correspondence should be addressed.

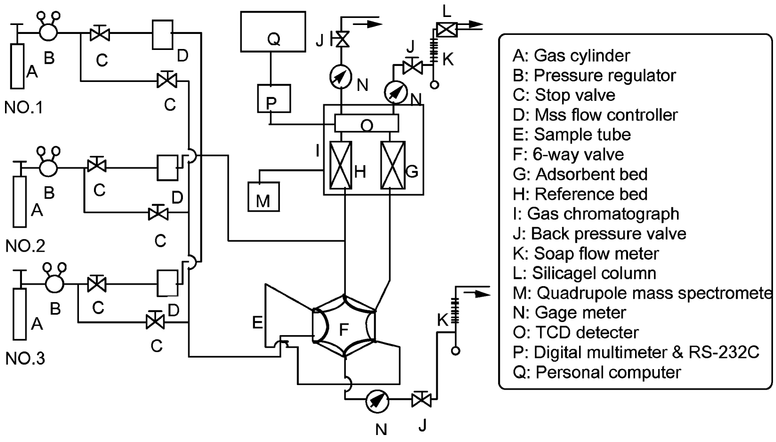

Figure 1. Experimental apparatus.

personal computer. Simulated chromatogram by a personal computer can be overlapped on experimental chromatogram shown in the monitor screen. Further, moment of pulse response, which is shown in the monitor screen, can be automatically calculated by the personal computer.

The first absolute moment and the second central moment were evaluated from the effluent peak $C_e(t)$ as follows:

$$\mu_1 = \int_0^\infty C_e(t)\, t dt \bigg/ \int_0^\infty C_e(t)\, dt \tag{1}$$

$$\mu_2' = \int_0^\infty C_e(t)(t-\mu_1)^2 dt \bigg/ \int_0^\infty C_e(t)\, dt \tag{2}$$

2.2. Moment Analysis

Basic equations are in ref. (Kumar et al., 1982).

The resultant moment equations of the impulse response are

$$\mu_1 = \frac{z}{u}\left\{1 + \frac{(1-\varepsilon)\rho_p(1-y)K^*}{\varepsilon}\right\} \tag{3}$$

$$\begin{aligned}\mu_2 &= \frac{2z}{u}\left[Ez\left\{\frac{1+(1-\varepsilon)\rho_p K^*}{\varepsilon u}\right\}^2 + \frac{(1-\varepsilon)\rho_p(1-y)K^*}{\varepsilon Ksav}\right] \\ &= \frac{2z}{u}(\delta_d + \delta_f + \delta_a + \delta_i)\end{aligned} \tag{4}$$

where μ_1 = first absolute moment of the chromatographic peak[s] μ_2 = second central moment[s^2].

$$\delta_d = \frac{Ez}{u^2}\left\{1 + \frac{(1-\varepsilon)\rho_p(1-y)K^*}{\varepsilon}\right\}^2 \tag{5}$$

$$\delta_f = \frac{1-\varepsilon}{\varepsilon}\frac{R}{3k_f}\rho_p^2(1-y)K^{*2} \tag{6}$$

$$\delta_a = \frac{1-\varepsilon}{\varepsilon}\frac{R^2}{15D_a}\rho_p^2(1-y)K^{*2} \tag{7}$$

$$\delta_i = \frac{1-\varepsilon}{\varepsilon}\frac{\rho_p(1-y)K^*}{15D}a^{-2}\exp(\sigma^2) \tag{8}$$

where K^* = apparent adsorption equilibrium constant, E_z = axial dispersion coefficient based on void spaces in the bed, k_f = external mass transfer coefficient, D_a = diffusivity in macropores and D = diffusivity in micropores based on amount adsorbed gradient driving force. The arithmetic average radius $\bar{a}$ is 8.2 μm (Chihara et al., 1978).

Equation (3) was used along with the experimental μ_1 to obtain the adsorption constant K^*. Equations (4) to (8) were used along with the experimental μ_2' to obtain the diffusivity in micropores D.

2.3. Stop & Go Simulation

Numerical solution for multi component chromatogram in time domain could be obtained by appropriate model equations with experimental conditions. This simulated chromatogram can be compared with experimental chromatogram to determine the equilibrium and the adsorption kinetic parameters. Here Markham-Benton equation as for adsorption equilibrium and linear driving force (LDF) approximation as for adsorption kinetics were adapted for numerical calculation, which was based on stop & go method (Chihara et al., 1986; Chihara and Kondo, 1986). In particular, LDF model of adsorption kinetics was based on non-equilibrium thermodynamics.

For binary adsorbates, adsorption rate equations are

$$\gamma \frac{\partial q_1}{\partial t} = Ksav_{1,1}(q_1^* - q_1) + Ksav_{1,2}(q_2^* - q_2) \quad (9)$$

$$\gamma \frac{\partial q_2}{\partial t} = Ksav_{2,1}(q_1^* - q_1) + Ksav_{2,2}(q_2^* - q_2) \quad (10)$$

where $Ksav$ = Overall mass transfer coefficients.

Overall mass transfer coefficients ($Ksav$) for LDF model were determined. Then, micropore diffusivities were obtained by subtracting other mass transfer effects from overall resistance ($\gamma/Ksav$). Thus obtained micropore diffusivities were correlated with chemical potential driving force by consideration of Fick's diffusion equation and non-equilibrium thermodynamics (Karger and Bulows, 1975).

$$\frac{D_{11}}{a^2} = \frac{D_1'}{a^2}\frac{\delta \ln p_1}{\delta \ln q_1} \quad (11)$$

$$\frac{D_{12}}{a^2} = \frac{D_1'}{a^2}\frac{q_2}{q_1}\frac{\delta \ln p_1}{\delta \ln q_2} \quad (12)$$

$$\frac{D_{21}}{a^2} = \frac{D_2'}{a^2}\frac{q_2}{q_1}\frac{\delta \ln p_2}{\delta \ln q_1} \quad (13)$$

$$\frac{D_{22}}{a^2} = \frac{D_2'}{a^2}\frac{\delta \ln p_2}{\delta \ln q_2} \quad (14)$$

For instance, $Ksav$ is related to D in single adsorbate case as

$$\frac{1}{Ksav} = \frac{a^2}{15D} + K^*\left(\frac{R}{3k_f} + \frac{R^2}{15\varepsilon D_a}\right) \quad (15)$$

For binary case, when using Eq. (15), apparent K^* could be determined by appropriate slope of adsorption isothermal plane at perturbation point.

3. Result and Discussion

3.1. Single Adsorbate Carrier Mixed with He and The Same Adosorbate Pulse

Figure 2 shows an example of comparison of experimental chromatogram with simulated chromatogram for MSC5A to obtain $Ksav$ for LDF model. Experimental conditions were 313 [K], column pressure 5 [atm], flow rate 25 [cm/sec] and He + CH_4 mixed gas carrier with CH_4 pulse. Here CH_4 concentration in the carrier gas was changed 40, 60 and 80 [%].

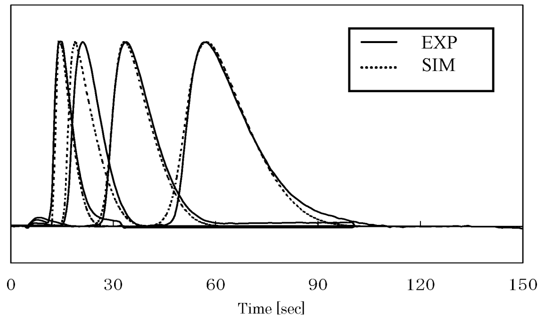

Figure 2. Comparison of experimental peaks with simulation.

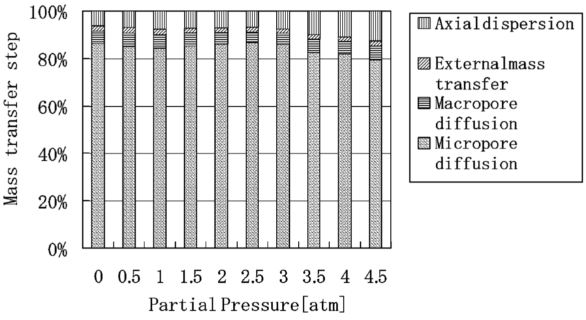

Figure 3. Mass transfer steps of N_2 on to MSC5A.

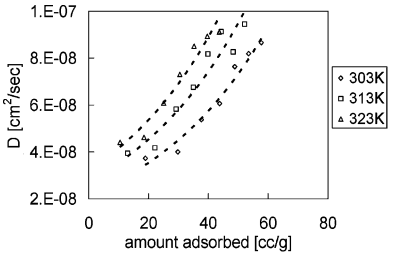

Figure 4. Dependency of micropore diffusivity coefficient on the amount adsorbed.

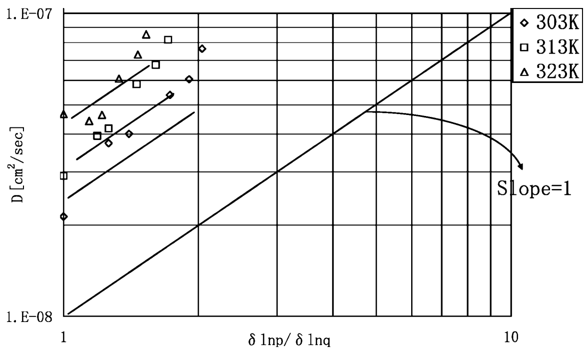

Figure 5. Correlation based on chemical potential driving force.

Figure 3 shows contribution of axial dispersion, external mass transfer, macropore diffusion and micropoore diffusion in case of N_2 for MSC5A. This figure illustrated that mass transfer is controlled by micropore diffusion.

Figure 4 shows the dependency of micropore diffusivity coefficient of CH_4 with amount adsorbed at 303, 313 and 323 [K] for MSC5A.

Figure 5 shows the correlation of micropore diffusivity of CH_4 with chemical potential driving force at 303, 313 and 323 [K] for MSC5A. Proportional relation was obtained, which means that micropore diffusion is based on chemical potential driving force.

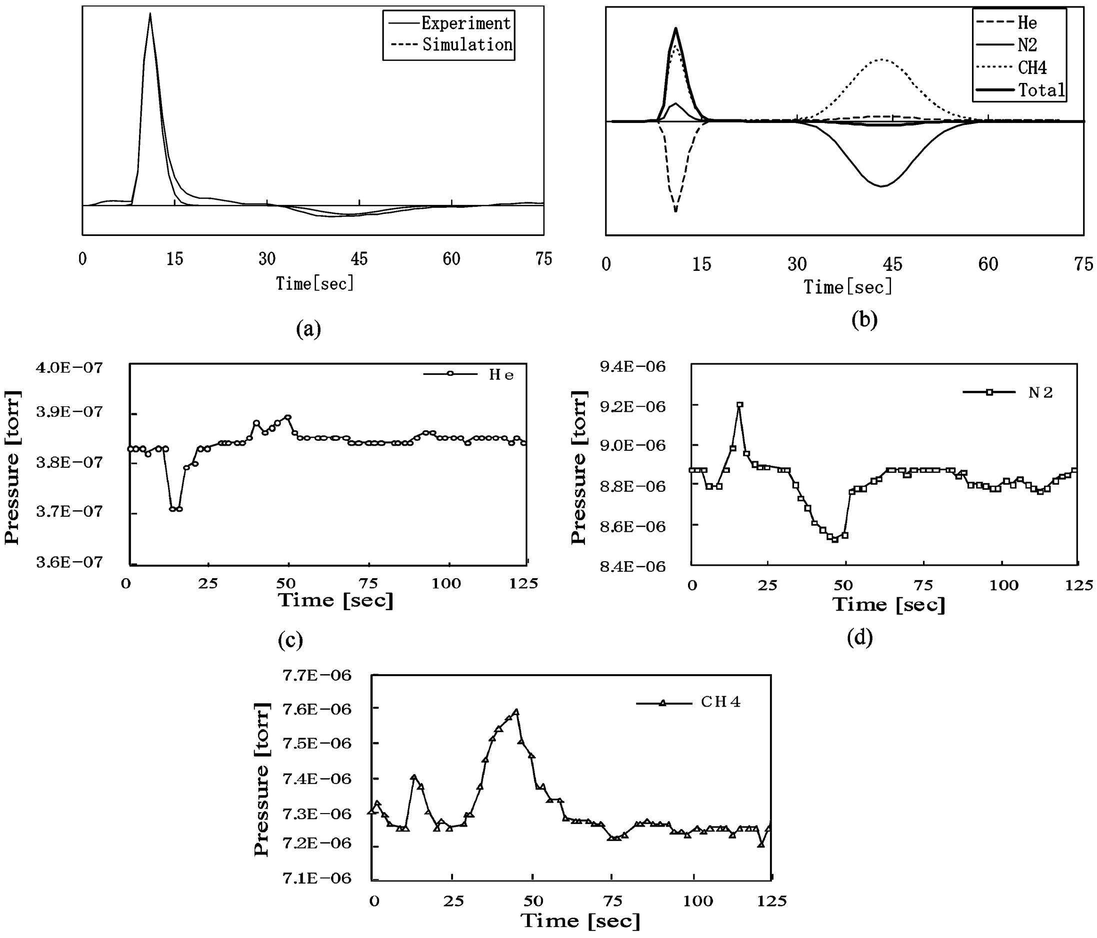

(a)
(b)
(c)
(d)
(e)

Figure 6. (a) Comparison between experimental chromatogram and simulated one, (b) Simulation of pulse response of each component, (c) Experimental peak of Helium by mass detector, (d) Experimental peak of N_2 by mass detector and (e) and Experimental peak of CH_4 by mass detector.

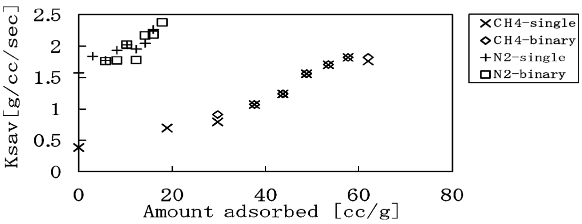

Figure 7. Comparison of K_{sav} of single adsorbate, and Ksav of binary adsorbate [He+ CH_4– N_2].

3.2. Binary Adsorbate Carrier Mixed with He and Adsobate Pulse

Figure 6(a) to (e) show experimental and simulation results in an example case of binary adsorbate carrier mixed with He and an adsorbate pulse for MSC5A. Experimental conditions were 323 [K], column pressure 5 [atm], flow rate 25 [cm/sec] and He(10%) + N_2(30%) + CH_4(60%) mixed gas carrier with N_2 pulse. Figure 6(a) is the comparison between experimental and simulated TCD peaks. Figure 6(b) is simulated peaks of each gas component and total peak. The total peak is assumed to be the sum of adsorbate peaks expect He and assumed to be as simulated TCD peak, which was found to be conincident with experiment as in Fig. 6(a). Figure 6(c) to (e) show experimental peaks of the components by mass detector. Each peaks in Fig. 6(b) could be compared to corresponding peak in Fig. 6(c) to (e) and to be found in good agreement. Simulated chromatogram for N_2 and CH_4 mixture may be regarded as co-diffusion or competitive adsorption for 1st peak and as counter-diffusion or displacement adsorption for 2nd peak.

Figure 7 shows comparison of Ksav obtained from single adsorbate system and binary adsorbates system. Both Ksav for N_2 and CH_4 for single experiment show dependencies on amount adsorbed itself. As for Ksav for binary adsorbate [He + CH_4 carrier + N_2 pulse], CH_4-binary shows reasonable dependency, same as single case. Here N_2-binary should remain constant, cause no amount adsorbed in the column. However, the Ksav for N_2 is affected by CH_4 adsorption, as if there is some N_2 amount adsorbed.

4. Conclusion

Good agreements between experimental chromatogram and simulated chromatogram, which were based on the modeling of Stop & Go method, were observed in case of peturbation chromatography with mixed adsorbate gas carrier. And micropore diffusivities obtained were interpreted by chemical potential driving force consideration based on non-equilibrium thermodynamics law. Some possibilitty was shown for cross effect of micropore diffusion in multicomponent adsorption.

References

Chihara, K. et al., "Simulation of Pressure Swing Adsorption for Air Separation," in *Proc. 7th Int. zeolite Conf.*, pp. 563, 1986.

Chihara, K. and A. Kondo, "Simulation of Pressure Swing Adsorption—Three Gas Components and Three Adsorption Columns-," 2nd FOA, 165 (1986).

Chihara, K., M. Suzuki, and K. Kawazoe, "Adsorption Rate on Molecular Sieving Carbon by Chromatography," *AIChE J.*, **24**, 237 (1978).

Karger, J. and M. Bulows, *Chem. Eng. Sci.*, **30**, 893 (1975).

Kumar, R., R.C. Duncan, and D.M. Ruthven, "A Chromatographic Study of Diffusion of Single Components and Binary Mixtures of Gases in 4A and 5A Zeolites," *Can. J. Chem. Eng.*, **57**, 342 (1982).

Ruthven, D.M, *Principle of Adsorption and Adsorption Process*, Wiley, p. 146, 1984.

Ruthven, D.M. and R. Kumar, "A Chromatographic Study of the Diffusion of N_2, CH_4 and Binary CH_4-N_2 Mixtures in 4A Molecular Sieve," *Can. J. Chem. Eng.*, **57**, 342 (1979).

Tondeur, D., H. Kabir, L. Luo, and J. Granger, "Multicomponent Adsorption Equilibria from Impulse Response Chromatography," *Chem. Eng. Science*, **51**(N15), 3781–3799 (1996).